Studying Neutral Hydrogen Shells in the Interstellar Medium

Elizabeth M. Tennyson, Dr. Shauna Sallmen

Department of Physics, University of Wisconsin - La Crosse, La Crosse, WI 54601

Dr. Eric J. Korpela

Space Sciences Laboratory, University of California at Berkeley, Berkeley, CA, 94720

ABSTRACT

One of the many processes that occur in our Milky Way Galaxy is the interaction of Neutral Hydrogen (H I) shells with the Interstellar Medium (ISM). H I shells are formed when material from stellar winds and supernova explosions expands outward and mixes with the ISM. Without this phenomenon the heavy elements made in stars would not be recycled and reused for future star and planet systems. The goal of this project is to better understand how interstellar shells evolve. To acquire a better grasp of a shell's characteristics and development, we compared images for 55 shells that were discovered in the Search for Extraterrestrial Neutral Hydrogen (SETHI) radio database. The SETHI images show cold, neutral gas, the H-Alpha Composite Survey images show warm, ionized gas, the IRIS (infrared) images show warm dust, and the RASS (X-ray) images reveal hot gas. The initial comparison identified nine potentially interesting shells. Of these, four are most suitable for detailed follow-up study, based on information available from their kinematic distances. We present a catalog of the shells we classified, including details of those that are likely targets. Follow-up detailed multi-wavelength comparisons can give us estimates on a shells's age and evolutionary status.

Subject headings: ISM: general — ISM: bubbles, ISM: supernova remnants

1. Introduction

Neutral Hydrogen (H I) shells are found throughout the Interstellar Medium (ISM) of our Milky Way Galaxy. These interstellar shells are formed by supernova explosions and stellar winds, which eject hot, ionized material. Over time, the ionized gases cool and become neutral gases. The materials that are dispersed from these events mix with the

surrounding ISM and enrich it with heavy elements like gold, silicon, and iron. This process is an important part of the stellar evolution cycle that leads to the formation of new stars and planetary systems. Examining these shells in detail will give a better understanding of both H I shells and interstellar processes in our Galaxy.

One way to analyze interstellar shells in more detail is to observe the distributions of material at different temperatures. Comparing images taken of a specific object at different wavelengths can reveal important characteristics of the expanding shell (e.g. Heiles, Haffner, & Reynolds 1999). At higher temperatures, higher energy radiation such as X-rays will be emitted. Lower energy radiation is an indication of cooler gas. It is expected that a young supernova remnant (SNR) will emit high energy radiation at its core because it would be very hot inside. The lower energy radiation will be emitted by cooler gas surrounding the object in question. As the SNR expands and cools, the distribution of hot and cold material changes. Therefore, using the information that different wavelengths can give, it is possible to determine the evolution of an object like an H I shell.

Recent radio surveys have allowed us to identify new H I shells. For example, the Search for Extraterrestrial H I (SETHI) database is based on 21-cm data taken at the Arecibo Radio Telescope in Puerto Rico. This survey maps the neutral hydrogen in our Galaxy at a higher resolution and sensitivity than previous efforts. These high-quality data have resulted in the discovery of new shells (e.g. Korpela et al. 2004).

In this project, images at multiple wavelengths are compared to better comprehend the morphology of shells recently discovered in a search of the SETHI data (Sallmen et al., in preparation). The wavelengths that were chosen (X-ray, Hα, infrared, and 21-cm) are emitted by gas at different temperatures in and around the H I shells. These four images compared to one another help identify shells suitable for more detailed study, and give information about the inter-workings of gas at various temperatures within such shells.

2. Methods

Searching the high-resolution SETHI data by eye resulted in a list of 55 potential new H I shells, including their location and size (Sallmen et al., in preparation). In order to view these shells at the wavelengths of interest, the public Astronomical Database *SkyView* was used (McGlynn et al. 1996). This database contains surveys in a variety of wavelengths. For each shell, appropriate regions of these data were extracted from *SkyView* for three surveys. (1) The ROSAT X-ray All Sky Survey corresponding to X-rays of approximately 1/4 keV (RASSband1 & RASSband2) was used to analyze the hot ($\sim 10^6$ K) X-ray emitting gas.

(2) The H-Alpha Composite Survey (Hα) was used to map the warm ($\sim$10,000 K), ionized hydrogen gas. (3) The Infrared Imaging Survey (IRIS) showed the warm infrared emitting dust that resides in and/or around the shell. The cold ($\sim$100 K) neutral hydrogen gas was shown in the SETHi data.

The program SAOImage ds9 was used to compare H I data versus data at other wavelengths. This software assisted with the comparison process because it enabled a viewer to blink through images as well as draw the same regions on multiple images. The correlations between images for each shell were examined and quantified. For example, if there were low H-Alpha emission levels in the same region as the low H I emissions, the images were correlated. Similarly, bright X-ray emissions within the region of low H I emissions represented a correlation between the two surveys. Such correlations make the shell more appropriate for further multi-wavelength analysis.

3. Results

We quantified such correlations for 55 shells in our list. The number 1 was assigned to shells where multiple correlations between multiwavelength images were easy to identify. The quantification number 3 denotes no identifiable correlation at all between survey images.

After quantifying the multi-wavelength correlations, 9 shells had a quality of 1, 23 had a quality of 2, and 23 had a quality of 3. The image set in Figure 1 shows shell GSH 034+20+011, which was assigned a quality of 1.

Each survey image of this shell GSH 034+20+011 is correlated to at least one of the other survey images it was compared with. The ionized hydrogen gas emissions in Figure 1b generally match the cold, neutral hydrogen emissions in Figure 1a. The detailed correlation will reveal where warm, ionized gas is cooling into neutral hydrogen near the edges of the shell. The warm, infrared dust (Figure 1c) is anti-correlated to the hot gas (Figure 1d) because the dust blocks some of the X-ray emissions from getting through. The presence of the warm dust causes the lack of X-ray emissions. The regions of slightly brighter X-ray emission (seen in Figure 1d) in the center of the interstellar shell suggest it may contain hot, X-ray emitting gas. Typically, young expanding shells contain X-ray emission. Faint or no X-ray emission indicates an older shell expanding more slowly.

GSH 034+20+011 – HI

GSH 034+20+011 – Halpha

GSH 034+20+011 – IRIS
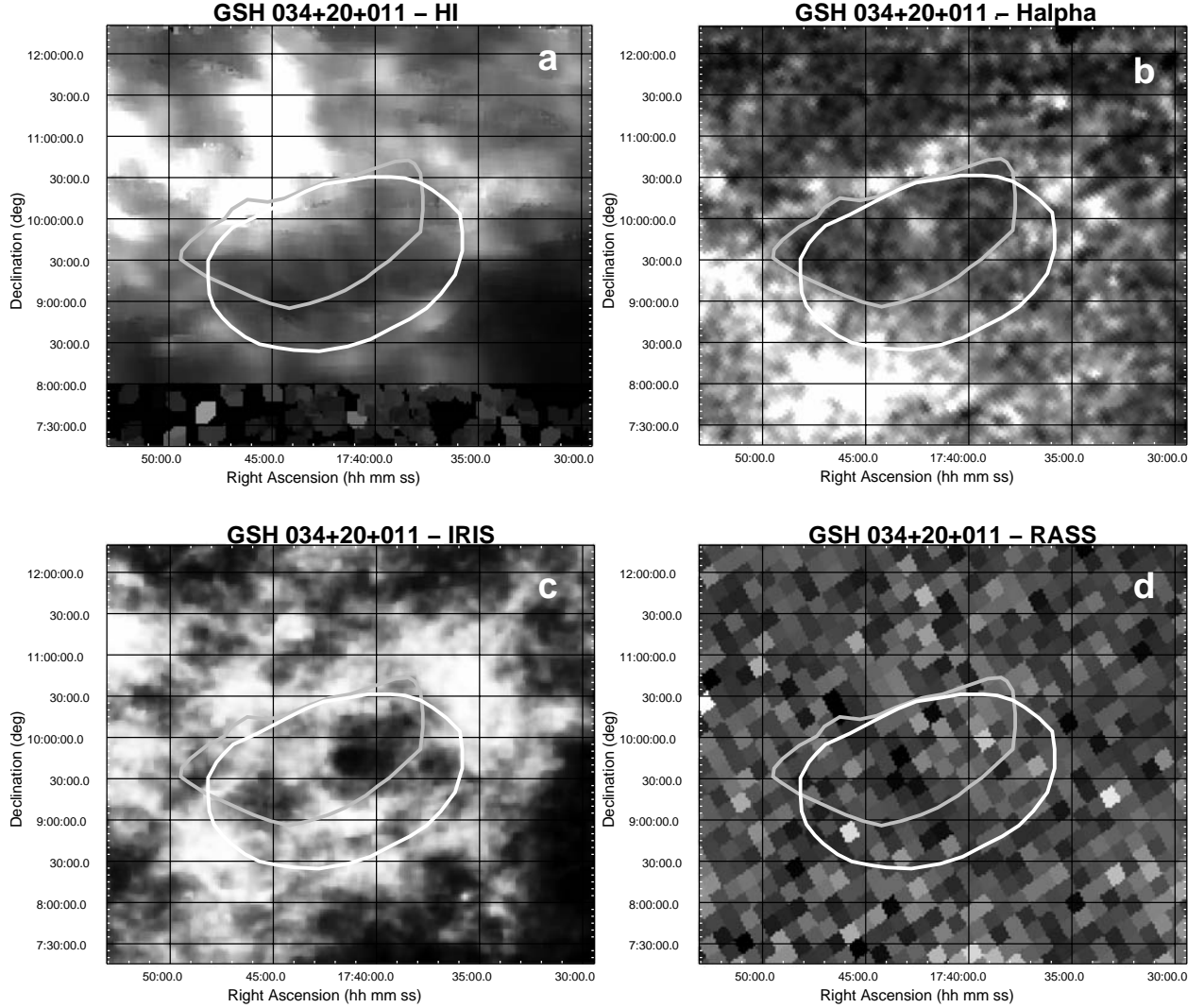
GSH 034+20+011 – RASS

Fig. 1.— Four images of shell GSH 034+20+011. (a) Neutral Hydrogen shell at 21-cm. The inner edges of the H I emission are outlined in white. This region is marked on all four images for comparison purposes. (b) H-Alpha Composite image. The inner edges of the H-Alpha emission are outlined in grey. This region is also marked in all four images for comparison purposes. The overlapping low-emission regions of the H-Alpha and H I images suggests a correlation between the warm ionized gas and the cold neutral gas in the shell. (c) IRIS 100 micro-meter Survey image of the same shell. The warm infrared emitting gas is less predominant in the H I hole region, and plentiful where the neutral and ionized hydrogen gases are plentiful. (d) RASSband1 and RASSband2 Survey images added together. Within the H I hole hot gas X-Ray emissions are weakest where the IR image suggests the presence of warm infrared dust.

Table 1: SETH I Quality 1 Shell Information

| Shell ID | α | δ | θ | ΔV |
GSH lll+bb+vvv	hh mm	°	°	km s^{-1}
GSH029+38+005	16 28	13.75	3.1	4.64
GSH034+20+011	17 42	9.5	2.8	10.83
GSH044+38+002	16 45	24.75	1.9	6.21
GSH114−54−005	00 30	8.5	N/A	9.28
GSH208+32+006	08 43	18	5.8	15.46
GSH213+28+012	08 34	12	3.7	12.38
GSH274+74−006	12 19	12.5	6.4	10.82
GSH294+76+000	12 43	13.25	4.1	9.28
GSH325+78−001	13 10	15.75	8.4	7.74

Table 1 lists the 9 H I shells that were identified based on the quality parameter as potentially interesting targets for follow-up studies. Table 2 lists the 23 H I shells that were classified as quality 2. These are shells that had some correlations between multiple wavelength images, but not as many as those in Table 1.

Tables 1 and 2 both give the same information for each shell. The Shell IDs in column 1 describe the location of the shell. The three characters immediately following the GSH letters represent the galactic longitude of the shell center. The next three characters represent the galactic latitude of the shell. The following four characters give the radial velocity ($V_{\rm ref}$) at which the feature is most "shell-like". Columns 2 and 3 give the shell's location in celestial coordinates (α, δ). The mean angular diameter (θ, column 4) for our shells was found by averaging the angular size of the longest and shortest diameters of each shell, correcting for the fact that a given $\Delta\alpha$ is closer together at higher declination. If the H I shell were oval, the long diameter would correspond with the major axis while the short diameter would correspond with the minor axis. ΔV, listed in column 5, is the difference between the maximum and minimum velocities at which the H I shell is visible and "shell-like". The center coordinates, velocity range ΔV, and mean angular diameter θ all come from the search in which the shells were first identified (Sallmen et al., in preparation).

Table 2.   Quality 2 Shell Information

Shell ID GSH lll+bb+vvv	α hh mm	δ °	θ °	ΔV km s^{-1}
GSH029+34+005	16 42	12.25	1.5	12.37
GSH030+67−006	14 33	23.5	3.3	7.55
GSH040+04+048	18 49	8.25	1.8	15.47
GSH042+21+019	17 50	17	12.0	10.83
GSH045+14+031	18 23	17	2.3	10.85
GSH054−00+003	19 31	18.25	N/A	7.76
GSH055+18−005	18 20	27.25	4.7	6.18
GSH062+04−102	19 35	27	N/A	7.74
GSH065−01−079	19 58	27.5	N/A	24.75
GSH110−35−034	00 05	26.5	4.1	15.46
GSH112−46−008	00 19	16.25	4.0	9.28
GSH116−49−006	00 34	13.5	2.7	4.64
GSH156−37−003	02 43	19	4.4	6.16
GSH180−31+020	04 00	10	3.3	9.28
GSH182−18+005	04 46	17.5	3.9	6.19
GSH187−12+012	05 18	16.5	9.0	9.28
GSH192+06−017	06 33	21	3.4	21.66
GSH196+10+008	06 57	19	5.2	6.18
GSH210+54−003	10 12	23.25	2.8	10.83
GSH221+60+000	10 45	19.25	2.9	6.19
GSH231+55−009	10 36	12.5	3.4	6.19
GSH236+75−008	11 51	20.25	1.2	9.28
GSH262+73+003	12 05	13.5	8.7	6.18

4. Discussion

For the Quality 1 shells presented in Table 1, we used the Galactic rotation curve of Brand & Blitz (1993) to estimate the shell distances and sizes. Such kinematic distances are calculated by using the Galactic rotation curve, which describes the assumed circular orbital velocity at different distances from the Galactic center. Depending on the direction and distance of the target, Galactic rotation produces a particular radial velocity for the object. Since the direction of the H I shells are known, we can use the equations for the kinematic distances to calculate how far away the Earth is from a shell. In the inner Galaxy, there are generally two possible solutions for the distance, resulting in a distance ambiguity. In addition, this method has limitations because the motions of objects in the Galaxy are more turbulent and complex than for simple circular motion (Brand & Blitz 1993).

Table 3: SETHI Kinematic Distances and Sizes

Shell ID	D_{ref}	D_{min}	D_{max}	Size
GSH lll+bb+vvv	kpc	kpc	kpc	pc
GSH029+38+005	0.50 or 18.3	0.06 or 17.9	0.92 or 18.7	27^{+23}_{-24} or 990^{+20}_{-30}
GSH034+20+011	0.84 or 14.2	0.29 or 13.7	1.36 or 14.7	41^{+25}_{-27} or 690^{+30}_{-20}
GSH044+38+002	15.5	15	0.47 or 15.9	< 16 or 51^{+2}_{-2}
GSH114−54−005	1.83	0.27	3.32	N/A
GSH208+32+006	1.10	N/A	2.58	110^{+150}_{-110}
GSH213+28+012	1.74	0.83	2.78	110^{+70}_{-60}
GSH274+74−006	N/A	N/A	7.9	< 890
GSH294+76+000	N/A	N/A or 15.7	13.3 or N/A	< 950 or > 1130
GSH325+78−001	1.95	N/A	9.43	290^{+1130}_{-290}

Table 3 lists the results. Column 1 is the Shell ID, and column 2 describes the distance D_{ref} corresponding to the reference velocity V_{ref}. Columns 3 and 4 give the minimum and maximum distance (D_{min} and D_{max}) to the shell based on the velocity range (ΔV) from Tables 1 and 2. The final column of Table 3 shows the size estimates for each shell that result from these distance estimates and the mean angular diameter θ from Tables 1 and 2. The quoted errors incorporated into this method are based on D_{min} and D_{max} resulting from the observed velocity range of the shell.

The maximum expected size for H I shells is 100 to 300 pc (Ehlerová & Palouš 2005). Shells with well-determined distances and sizes are more suitable for further study because

this allows more accurate modeling of the energy requirements for shell evolution. The four shells listed in bold in Tables 1 and 3 are those that were selected as most interesting, because their kinematic distances are relatively well-constrained and yield reasonable sizes. This is assuming that the nearby distances and inferred sizes in Table 3 are correct.

5. Conclusions & Future Work

Based on examining 55 shells, four of our shells were identified as excellent candidates for follow-up studies. These would include more detailed multiple wavelength comparisons and modeling the H I shells' properties and evolution. In addition, seven shells were identified in the SETHI data that have not yet been examined for multi-wavelength correlations.

Acknowledgements

REFERENCES

Brand, J. & Blitz, L. 1993, A&A, 275, 67

Ehlerová, S., & Palouš, J. 2005, A&A, 437, 101

Heiles, C., Haffner, L.M., & Reynolds, R.J. 1999, *The Eridanus Superbubble in its Multi-wavelength Glory* in *ASP Conf.* series 168, 211, Ed. A.R. Taylor, T.L. Landecker & G.Joncas (San Francisco: ASP, 1999)

Korpela, E. et al. 2004, ASSL Volume. 315 *How Does the Galaxy Work*, 97

McGlynn, T., Scollick, K. & White, N. 1996, *SkyView: The Multi-Wavelength Sky on the Internet* in *IAU Symposium No. 179, New Horizons from Multi-Wavelength Sky Surveys*, 465, Ed. B.J. McLean et al. (Kluwer, 1996).